International Immunopharmacology 75 (2019) 105782

Contents lists available at ScienceDirect

International Immunopharmacology

journal homepage: www.elsevier.com/locate/intimp

Naringin mitigates myocardial strain and the inflammatory response in sepsis-induced myocardial dysfunction through regulation of PI3K/AKT/NF-κB pathway

Li-juan Sun[a,b], Wei Qiao[a], Yang-jie Xiao[a], Li Cui[a], Xin Wang[a], Wei-dong Ren[a,*]

[a] Department of Ultrasound, Shengjing Hospital of China Medical University, Shenyang 110004, PR China
[b] Department of Ultrasound, The First Hospital of Qinhuangdao, Qinhuangdao 066000, PR China

ARTICLE INFO

Keywords:
Naringin
Sepsis
Myocardial dysfunction
Layer-specific strain
PI3K/AKT/NF-κB signaling pathway

ABSTRACT

Sepsis-induced myocardial dysfunction (SIMD) is a manifestation of severe sepsis and is the main cause of increased mortality in sepsis patients. Naringin (Nar) has been reported to possess various biological activities and pharmacological properties. Therefore, the present study was undertaken to evaluate whether Nar can protect rats from the effects of LPS-induced SIMD. SD Rats were pre-treated with Nar (50 and 100 mg/kg) for 7 days before administration of a single dose of LPS (10 mg/kg, i.p.) on the seventh day. We found that Nar treatment markedly improved the global strain and strain rate of longitudinal, circumference, and radial direction (GLS/GLSr, GCS/GCSr, GRS/GRSr) compared to the LPS group. The layer-specific strain decreased gradually from the endocardial layer to epicardial layer, and the most serious damage occurred in the endocardial layer. Moreover, Nar significantly decreased the levels of pro-inflammatory cytokines (TNF-α, IL-1β, and IL-6) and myocardial enzymes (CK, LDH, and AST) induced by LPS and attenuated the inflammation response. Finally, Nar also inhibited NF-κB nuclear translocation and the activity of iNOS in H9c2 cardiomyocytes by activating PI3K/AKT signaling pathway. These results suggest that naringin may possess novel therapeutic potential for protection against LPS-induced myocardial dysfunction.

1. Introduction

Sepsis is a life-threatening organ dysfunction caused by an imbalanced response to an infection by the host [1]. Sepsis-induced myocardial dysfunction (SIMD) is a typical manifestation of severe sepsis and increases the mortality rate of sepsis patients [2]. SIMD can manifest in multiple ways, including elevation of myocardial injury markers, abnormal cardiac function, and hemodynamic instability [3]. The mortality rate of sepsis patients with myocardial dysfunction is 70–90%, compared to 20% in sepsis patients without myocardial damage [4]. Therefore, development of novel drugs for the treatment of SIMD is crucial.

Naringin (Nar, Fig. 1) is a natural flavonoid compound that is derived from rutaceous plants, such as grapefruit, oranges, and tangerines. Nar is also one of the main active components of Chinese herbal medicines, including drynaria rhizome, fructus aurantii and orange peel [5]. Intake of food rich in flavonoids is negatively correlated with the incidence and mortality of cardiovascular diseases [6]. Nar has been reported to possess various biological activities and pharmacological properties, including antioxidant, anti-inflammatory, anti-hypertensive, and anti-atherosclerosis effects, etc. [7–9]. Previous studies suggest that Nar can effectively protect the myocardium from ischemia reperfusion or high glucose injury by regulating the inflammatory response [10,11]. Moreover, Liu et al. reported that Nar can protect against LPS-induced cardiac injury in mice through its anti-inflammatory, anti-oxidant, and anti-apoptotic properties [12]. However, none of the previous studies have elucidated the underlying mechanisms through which Nar protects against cardiac injury. This is the first study focused on the potential effect of Nar on myocardial injury via the PI3K/AKT/NF-κB pathway in vivo and in vitro.

Previous studies have shown that the transcription factor nuclear factor kappa B (NF-κB) plays a key role in the pathogenesis of septic myocardial dysfunction [13]. NF-κB is a crucial nuclear transcription factor and controls the expression of many inflammatory genes. However, it is unclear whether the NF-κB signaling pathway is modulated by Nar in the context of SIMD. The phosphatidylinositol 3-kinase (PI3K)-protein kinase B (AKT) pathway is an important cellular cascade involved in the response to external stimuli [14]. The PI3K activates the

* Corresponding author.
E-mail address: renweidong3@163.com (W.-d. Ren).

https://doi.org/10.1016/j.intimp.2019.105782
Received 6 April 2019; Received in revised form 18 July 2019; Accepted 24 July 2019
Available online 31 July 2019

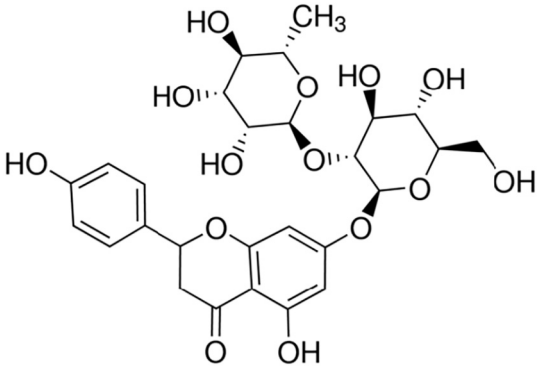

Fig. 1. Molecular formula of naringin (Nar).

downstream signaling molecule AKT, and plays an important role in a wide variety of biological responses, including inflammation, cellular proliferation, and apoptosis, all of which may be involved in cardiac diseases [15]. Therefore, elucidating the signaling pathways which are activated by Nar could provide detailed information about the mechanism through which it protects against cardiac injury.

Speckle Tracking Echocardiography (STE) is a novel echocardiographic imaging technique for evaluating myocardial function that is not thought to be affected by the preload and afterload. Unlike conventional ultrasound indexes, STE has greater sensitivity in detecting early myocardial dysfunction [16]. Layer-specific myocardial strain can be used to analyze the inner, middle, and outer layers of the ventricular wall to evaluate segmental and global functions of myocardium. This technique has been tested in many different cardiovascular diseases [17,18]. However, no studies have evaluated the longitudinal strain (LS) and circumferential strain (CS) of the three layers of the left ventricle in SIMD rats.

In this study, we evaluated the effects of naringin on global and layer-specific strain in SIMD rats, and we elucidated the underlying mechanism of its cardiac protective effect. Overall, these studies provide an experimental basis for the use of naringin treatment for SIMD.

2. Materials and methods

2.1. Reagents

Escherichia coli LPS (O111:B4) and naringin (≥95% purity) were purchased from Sigma-Aldrich (St. Louis, MO, USA). Dexamethasone sodium phosphate (Dexa) was purchased from MeiLun Biology Technology Co., Ltd. (Dalian, China).

2.2. Animals

Adult male Sprague-Dawley (SD) rats (weight: 300 ± 5 g, age: 8w–9w) from Huafukang Bioscience Co., Ltd. (Beijing, China) were raised in a specific pathogen free (SPF) laboratory under a 12 hour/12 hour light/dark cycle at 22–24 °C and a humidity of 70% (Certificate number: SYXK (Liao) 2017-0004). The experimental protocols were approved by the Animal Care and Use Committee of Shengjing Hospital of China Medical University. All of the rats were adapted to the environment for 1 week, and then they were randomly assigned into five groups (n = 15 for each group): 1) the control group, which was administered sterile saline; 2) the LPS group, which was intraperitoneally injected with LPS (10 mg/kg, a dose that ensured cardiac insufficiency without mortality [19,20]); 3) the LPS + Nar (50 mg/kg) group; 4) the LPS + Nar (100 mg/kg) group. Nar (≥95% purity, Sigma-Aldrich, St. Louis, MO, USA) was administered by oral gavage (50 or 100 mg/kg/day) for seven days [12,21]. About 1 h after the last administration on the seventh day, the LPS and LPS + Nar groups were intraperitoneally injected with LPS. The control group received sterile saline only. In this experiment, Dexa (2 mg/kg) was used as a positive control and was injected intraperitoneally 1 h before LPS challenge [22]. Six hours after LPS administration, the rats were anesthetized with pentobarbital sodium before other procedures were performed.

2.3. Conventional echocardiography

Images were obtained using a GE Vivid E9 ultrasound machine (GE Healthcare, Horten, Norway) equipped with a 12S transducer, frequency 9–12 MHz. Rats were scanned in a left decubitus position 6 h after LPS injection. The dimensions of the left ventricular end-diastolic (LVEDd) and end-systolic diameters (LVEDs), end-diastolic volume (EDV), end-systolic volume (ESV), left ventricular ejection fraction (LVEF), and fractional shortening (FS) were measured from M-Mode in the parasternal long-axis view. All the parameters were measured three times, and the mean value was calculated.

2.4. Speckle Tracking Echocardiography (STE)

All the images were analyzed using an offline workstation (EchoPAC, PC Version: 201). The contours of the epicardium and endocardium were aligned manually to match areas of interest (ROI) to the actual thickness of the ventricular wall. The left ventricular wall was automatically divided into three separate myocardial layers, allowing for assessment of longitudinal or circumferential endocardial, mid-myocardial, and epicardial strain. All segmental values from the long-axis or short-axis view were averaged to ventricular global strain. The cardiac STE measurements of LV were as follows: global longitudinal strain/strain rate (GLS/GLSr); longitudinal strain in the endocardial layer (LS-endo), the mid-myocardial layer (LS-mid), and the epicardial layer (LS-epi); global circumferential strain/strain rate (GCS/GCSr); circumferential strain in the endocardial layer (CS-endo), the mid-myocardial layer (CS-mid), and the epicardial layer (CS-epi); and global radial strain/strain rate (GRS/GRSr). All images were analyzed three times by two independent investigators.

2.5. Biochemical analysis

After the examination of the echocardiograph, whole blood was collected and centrifuged in order to obtain the serum. The creatine kinase (CK), lactate dehydrogenase (LDH), and aspartate aminotransferase (AST) levels in serum were determined using an automatic biochemical analyzer (IDEXX Laboratories Inc., Maine, USA). The protein level of tumor necrosis factor α (TNF-α) in serum was measured by ELISA (R&D Systems, Minneapolis, MN, USA), which was done according to the manufacturer's instructions.

2.6. Histopathological examination

The effects of Nar on heart histopathology were determined by hematoxylin and eosin (H&E) staining. The harvested heart tissue samples were fixed in 10% neutral formalin and embedded in paraffin. Then, the samples from the left ventricle were cut into sections (4 μm) and stained with H&E. Finally, the sections were examined under a light microscope (Nikon, Tokyo, Japan). Each section was given a histopathologic score according to the degree of damage between 0 and 4: 0 (< 10%), 1 (10–25%), 2 (25–50%), 3(50–75%), and 4 (> 75% involvement) [23].

2.7. Myeloperoxidase (MPO) activity assay

The myocardial tissues obtained from each group were made into homogenates and were used to determine MPO activity using the MPO activity assay (Jiancheng Bioengineering Institute, Nanjing, China). The test was performed according to the manufacturer's instructions.

2.8. Immunohistochemistry (IHC)

Heart tissue sections were dewaxed sequentially in xylene and graded ethanol. Antigen retrieval was assayed using antigen retrieval buffer at 37 °C for 30 min, and the samples were incubated with diluted primary antibody against NF-κB p65 (1:100 dilution; Proteintech, Chicago, USA) at 4 °C overnight. The samples were then incubated with a biotinylated secondary antibody for 30 min at room temperature. The sections were colored with DAB at room temperature in the dark, and the nuclei were counterstained with hematoxylin. Finally, the heart tissue sections were dehydrated sequentially with graded ethanol and xylene. The expression of NF-κB p65 in the five groups was scored as previously described [24].

2.9. Cell culture and treatment

Rat H9c2 cardiomyocytes (Cell bank of the Chinese Academy of Sciences, Shanghai, China) were cultured in high glucose DMEM (Biological Industries, Kibbutz Beit-Haemek, Israel) containing 10% fetal bovine serum (FBS; Biological Industries, Kibbutz Beit-Haemek, Israel) and 1% antibiotics (100 IU/ml penicillin and 100 mg/ml streptomycin). The cells were maintained at 37 °C in a humidified incubator with 5% CO_2. The H9c2 cells were pretreated with Nar (40/80 μM) 1 h before LPS treatment [25]. Dimethyl sulphoxide (DMSO)-treated cells (0.1%) were used as a vehicle control. LY294002 (10 μM) (Cell Signaling Technology, Beverly, MA, USA), a specific PI3K inhibitor [26], was used to determine if the PI3K/AKT/NF-κB signaling pathway was involved in naringin's action on LPS-induced H9c2 cardiomyocytes.

2.10. CCK-8 assay

Cell viability was determined using the Cell Counting Kit-8 (CCK-8) assay (Dojindo, Kumamoto, Japan). Various concentrations of Nar (10–320 μM) were added to the wells. After a 1 hour treatment, the cells were incubated in the presence or absence of LPS (10 μg/ml) for 24 h [15]. Next, 10 μl of CCK-8 reagent was added to each well and allowed to incubate at 37 °C for 2 h. The absorbance was measured at 450 nm using a microplate reader. The absorbance reading of the background control was subtracted from each experimental absorbance reading.

2.11. Real-time PCR

Total RNA was extracted from H9c2 cardiomyocytes and heart tissue using Trizol reagent (Takara, Shiga, Japan) according to the manufacturer's protocol. 1 microgram of total RNA was reverse-transcribed into cDNA using a Reverse Transcription kit (Takara, Shiga, Japan) with the primer oligo dT. The oligonucleotide primers (Sangon Biotechnology, Shanghai, China) were as follows: TNF-α: forward 5′-GCA TGA TCC GAG ATG TGG AAC TGG-3′ and reverse 5′-CGC CAC GAG CAG GAA TGA GAA G-3′; IL-6: forward 5′-AGG AGT GGC TAA GGA CCA AGA CC-3′ and reverse 5′-TGC CGA GTA GAC CTC A AG TGA CC-3′; iNOS: forward 5′-GAG ACG CAC AGG CAG AGG TTG-3′ and reverse 5′-CAG GAA GGC AGC AGG CAC AC-3′; IL-1β: forward 5′-CAG CAG CAC ATC AAC AAG AG-3′ and reverse 5′-CAG CAG GTT ATC ATC ATC ATC C-3′ and GAPDH: forward 5′-GGG TGT GAA CCA CGA GAA AT-3′ and reverse 5′-CCA CAG TCT TCT GAG TGG CA-3′. Quantitative real-time PCR was carried out using SYBR Premix Ex Taq II (Takara, Shiga, Japan) and a Light Cycler 480 system (Roche, Basel, Switzerland) as previously described [27]. The mRNA levels were analyzed using the $2^{-\triangle\triangle CT}$ method and normalized to the housekeeping gene GAPDH.

2.12. Western blot analysis

Total proteins were extracted from H9c2 cardiomyocytes using radioimmunoprecipitation assay (RIPA) Lysis Buffer (Beyotime, Shanghai, China). The Minute™ cytoplasmic and nuclear extraction kit (Invent Biotechnologies, Beijing, China) was used for the extraction of nuclear and cytosolic fractions according to the manufacturer's instructions. The protein concentration was measured using the enhanced BCA protein assay kit (Beyotime, Shanghai, China). Equal amounts of proteins were subjected to sodium dodecyl sulfate polyacrylamide gel electrophoresis (SDS-PAGE) in a 10% gel and transferred onto PVDF membranes (Millipore, Bedford, MA, United States). The membranes were blocked with 5% skim milk for 2 h at room temperature. The membrane were then incubated with primary antibodies against iNOS (1:1000 dilution; Abcam, San Diego, CA, USA), p-NF-κB p65 (1:5000 dilution; Abcam, San Diego, CA, USA), NF-κB p65 (1:1000 dilution; Proteintech, Chicago, USA), IkBα (1:1000 dilution; Cell Signaling Technology, Beverly, MA, USA), p-IkBα (1:1000 dilution; Cell Signaling Technology, Beverly, MA, USA), β-actin (1:10000 dilution; Proteintech, Chicago, USA), and histone H3 (1:2000 dilution; Proteintech, Chicago, USA) overnight at 4 °C. Finally, the blots were incubated with horseradish peroxidase (HRP)-conjugated secondary antibody and visualized using a GE Amersham Imager 600 (GE Healthcare Life Sciences, Pittsburgh, PA, USA) [28]. β-Actin and histone H3 were used as a cytoplasm and nuclear loading control, respectively.

2.13. Statistical analysis

Values are represented as mean ± standard deviation (SD). Data were analyzed using SPSS 19.0 software (SPSS Inc., Chicago, IL, USA). Comparisons of findings among different groups were analyzed by one way analysis of variance (ANOVA). $P < 0.05$ was considered statistically significant.

3. Results

3.1. Conventional echocardiography

In the LPS group, the LVEF and FS significantly decreased after LPS administration, and the LVEDd, LVEDs, EDV, and ESV increased compared to the control group ($P < 0.05$). In the LPS + Nar_{50} group, the LVEDd, EDV, and ESV all decreased compared to the LPS group. However, there were no significant changes in LVEDs, LVEF, and FS between the LPS + Nar_{50} group and the LPS group ($P > 0.05$). Conventional echocardiography parameters improved significantly in both the LPS + Nar_{100} group and the Dexa group. These results show that pretreatment with Nar effectively improves cardiac function in a dose-dependent manner (Table 1).

3.2. Changes in global strain/strain rate and layer-specific myocardial strain

In the LPS group, the left ventricular dysfunction parameters assessed by STE were already significantly reduced at the early timepoint compared to the control group. In LPS + Nar_{50} group, the GLS, GLSr and GCS were increased compared to the LPS group, but the GCSr and GRS, GRSr did not differ significantly. In LPS + Nar_{100} and LPS + Dexa group, all of the global strain and strain rates were dramatically elevated compared to the LPS group. The GCS, GCSr, GRS, and GRSr in the high dose group were significantly increased compared to the low-dose group (Fig. 2).

The changes in the three-layer longitudinal and circumferential strain parameters of the LV among the five groups are summarized in Table 2. Comparison analysis of layer-specific STE between groups showed that there was a significant reduction in LPS group (Fig. 3). Layer-specific STE analysis of the myocardial deformation revealed that the myocardial strain decreased gradually from endocardial layer to epicardial layer (LS-endo→ LS-epi, CS-endo→ CS-epi), with the highest value in endocardial layer and the lowest value in epicardial layer. The values of LS-endo, LS-mid, LS-epi, CS-endo, CS-mid, and CS-epi were

Table 1
Comparison of conventional echocardiographic indicators among groups.

Parameters	Control	LPS	LPS + Nar_{50}	LPS + Nar_{100}	LPS + Dexa
LVEDd(mm)	5.52 ± 0.54	6.17 ± 0.83*	5.63 ± 0.70#	5.36 ± 0.58##	5.44 ± 0.75##
LVEDs(mm)	2.78 ± 0.40	3.62 ± 0.36**	3.40 ± 0.34	2.94 ± 0.37##,△△	2.86 ± 0.35##,△△
EDV(ml)	0.41 ± 0.11	0.59 ± 0.08**	0.46 ± 0.11##	0.42 ± 0.11##	0.45 ± 0.11##
ESV(ml)	0.06 ± 0.02	0.12 ± 0.04**	0.10 ± 0.02#	0.07 ± 0.02##,△△	0.07 ± 0.03##,△
LVEF(%)	84.86 ± 3.36	71.71 ± 5.84**	75.82 ± 4.81	81.99 ± 6.28##,△	83.36 ± 4.00##,△△
FS(%)	45.49 ± 4.57	37.68 ± 4.77**	40.69 ± 2.63	44.19 ± 5.56#	42.57 ± 5.27##,△

Data were given as mean ± SD. LVEDd: left ventricular end-diastolic diameter; LVEDs: left ventricular end-systolic diameter; EDV: end-diastolic volume; ESV: end-systolic volume; LVEF: left ventricular ejection fraction; FS: fractional shortening.
* $P < 0.05$.
** $P < 0.01$ vs. the control group.
# $P < 0.05$.
$P < 0.01$ vs. the LPS group.
△ $P < 0.05$.
△△ $P < 0.01$ vs. the LPS + Nar_{50} group.

decreased by 43.13%, 42.29%, 40.98%, 47.16%, 46.91%, and 43.82% in LPS group versus the control group, respectively. In contrast, all of the parameters in the LPS + Nar groups (50 and 100 mg/kg) and LPS + Dexa group increased compared to the LPS group, except for CS-epi in the low dose group.

3.3. Effect of Nar on myocardial histology

In the control group, H&E staining revealed that the cardiomyocytes were normal, healthy, and well aligned (Fig. 4A). In contrast, LPS-treated rats exhibited myocardial cell edema, inflammatory cell infiltration, and widening of the intercellular space (Fig. 4B). Notably, Nar treatment markedly alleviated the aforementioned pathological changes, especially in the high-dose group (Fig. 4C and D). Dexa-treated rats showed significant attenuation of cardiac injuries compared to the LPS group, with relatively normal heart structure and conspicuous reduction in the accumulation of inflammatory cells (Fig. 4E). As shown in Fig. 4F, LPS stimulation markedly increased the histopathology score, but the score significantly decreased after treatment with Nar and Dexa.

3.4. Effect of Nar on MPO activity during LPS-induced SIMD

MPO activity serves as an indicator of neutrophils aggregation at the site of inflammation. As shown in Fig. 5, LPS treatment induced a large increase in MPO activity in the myocardial tissue in comparison to the

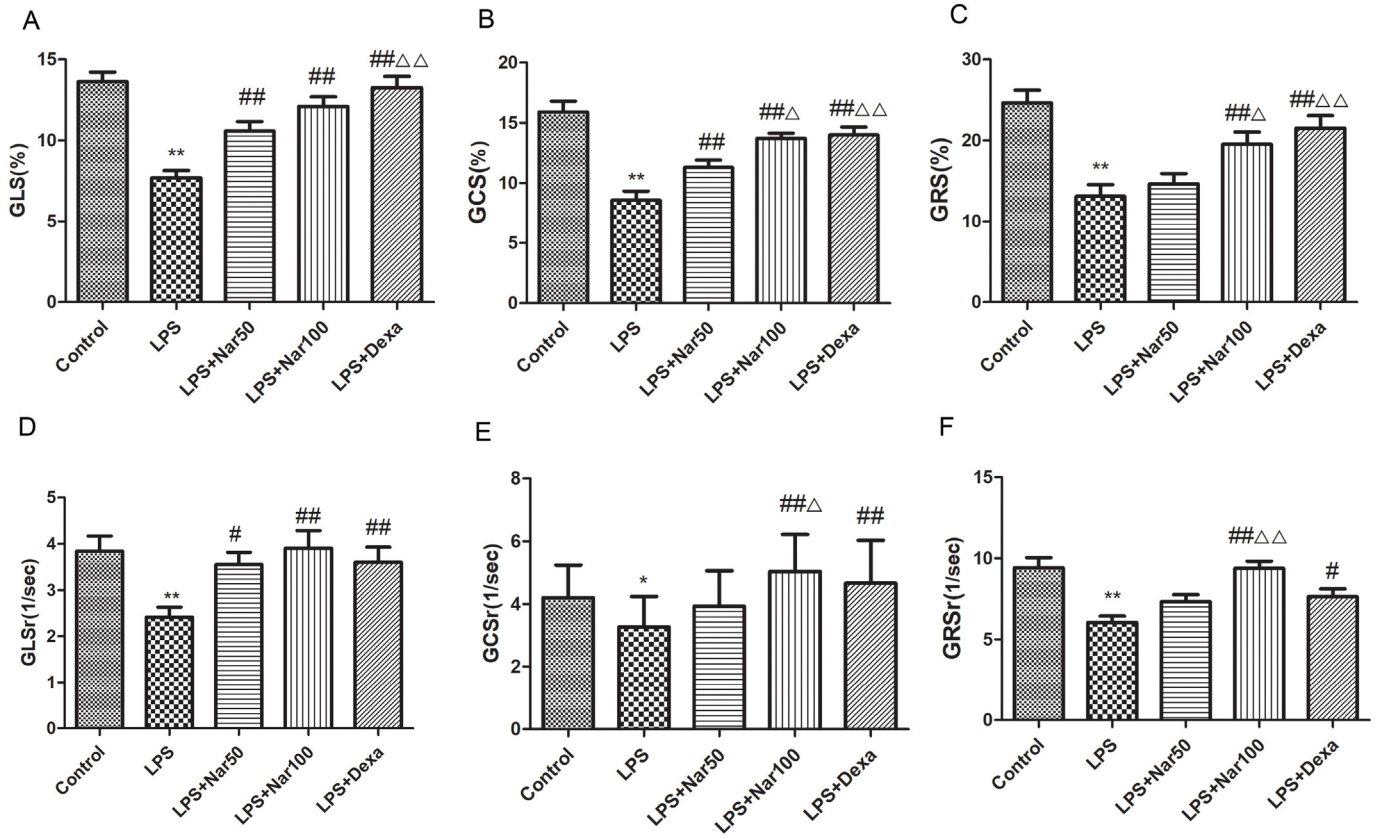

Fig. 2. The effect of Nar on myocardial global strain and strain rate in SIMD rats. GLS/GLSr: global longitudinal strain/strain rate; GCS/GCSr: global circumferential strain/strain rate; GRS/GRSr: global radial strain/strain rate. Data were presented as mean ± SD in absolute values. $^{*}P < 0.05$, $^{**}P < 0.01$ vs. control group; $^{\#}P < 0.05$, $^{\#\#}P < 0.01$ vs. LPS group; $^{\triangle}P < 0.05$, $^{\triangle\triangle}P < 0.01$ vs. LPS + Nar_{50} group.

Table 2
Effect of Nar on LV layer-specific LS and CS in SIMD rats.

Parameters	Control	LPS	LPS + Nar_{50}	LPS + Nar_{100}	LPS + Dexa
LS-endo (%)	−16.95 ± 3.37	−9.64 ± 2.45*	−13.58 ± 2.39#	−15.35 ± 3.51#	−15.67 ± 3.20#
LS-mid (%)	−13.62 ± 4.15&	−7.86 ± 2.17*,&	−10.43 ± 3.45#,&	−11.72 ± 3.81#,&	−13.52 ± 3.80#
LS-epi (%)	−10.25 ± 3.18&,$	−6.05 ± 2.42*,&,$	−8.26 ± 2.79#,&,$	−9.57 ± 2.70#,&	−10.61 ± 3.51#,△,&,$
CS-endo (%)	−21.97 ± 5.88	−11.61 ± 3.29*	−16.75 ± 5.52#	−19.69 ± 6.35#	−19.57 ± 6.18#
CS-mid (%)	−14.26 ± 2.88☆	−7.57 ± 3.26*,☆	−10.01 ± 2.94#,☆	−12.99 ± 2.90#,△,☆	−12.89 ± 3.50#,△,☆
CS-epi (%)	−8.01 ± 2.80☆,★	−4.50 ± 2.01*,☆,★	−6.13 ± 1.68☆,★	−8.42 ± 3.21#,☆,★	−8.16 ± 2.39#,☆,★

Data were given as mean ± SD. LS-endo: Longitudinal strain in the endocardial layer; LS-mid: Longitudinal strain in the mid-myocardial layer; LS-epi: Longitudinal strain in the epicardial layer; CS-endo: Circumferential strain in the endocardial layer; CS-mid: Circumferential strain in the mid-myocardial layer; CS-epi: Circumferential strain in the epicardial layer. Data were given as mean ± SD.

* $P < 0.05$ vs. the control group.
# $P < 0.05$ vs. the LPS group.
△ $P < 0.05$ vs. the LPS + Nar_{50} group.
& $P < 0.05$ vs. LS-endo in the same group.
$ $P < 0.05$ vs. LS-mid in the same group.
☆ $P < 0.05$ vs. CS-endo in the same group.
★ $P < 0.05$ vs. CS-mid in the same group.

control group. However, this increase was significantly inhibited by Nar in a dose dependent manner.

3.5. Effects of Nar on the levels of CK, LDH, AST, and TNF-α in serum

To observe the effect of Nar on the levels of myocardial enzymes and TNF-α protein in vivo, serum was collected from rats after LPS administration. The levels of CK, LDH, AST, and TNF-α in the serum dramatically increased in the LPS group. In contrast, Nar and Dexa treatments effectively decreased the levels of all five myocardial injury markers in a dose-dependent manner (Fig. 6).

3.6. Effects of Nar on H9c2 cardiomyocytes viability

The effect of Nar on cell viability was determined using the CCK-8 assay. As shown in Fig. 7, 10–320 μM Nar did not affect cell viability. LPS treatment for 24 h decreased cell viability to 62.33% ± 0.02%. However, pretreatment with Nar (40–320 μM) significantly protected H9c2 cardiomyocytes from insults induced by LPS.

3.7. Nar inhibited TNF-α, IL-1β, IL-6, and iNOS mRNA expression in vivo and in vitro

In LPS-treated SIMD rats, mRNA expression of TNF-α, IL-1β, IL-6, and iNOS increased significantly compared to the control group. However, pretreatment with Nar and Dexa significantly decreased TNF-α, IL-1β, IL-6, and iNOS expression compared to the LPS group ($P < 0.05$) (Fig. 8A).

H9c2 cardiomyocytes were pre-treated with Nar (40/80 μM) for 1 h and then stimulated with LPS (10 μg/ml) for 24 h. As shown in Fig. 8B, the mRNA expressions of TNF-α, IL-1β, IL-6, and iNOS in the LPS group were increased compared to the control group. As expected, treatment with Nar significantly reduced the levels of TNF-α, IL-1β, IL-6, and iNOS.

3.8. Nar improved cardiac function through PI3K/AKT/NF-κB pathway

The expression of NF-κB P65 (Fig. 9) in the heart tissue of rats 6 h after LPS stimulation was detected by IHC staining. The NF-κB P65

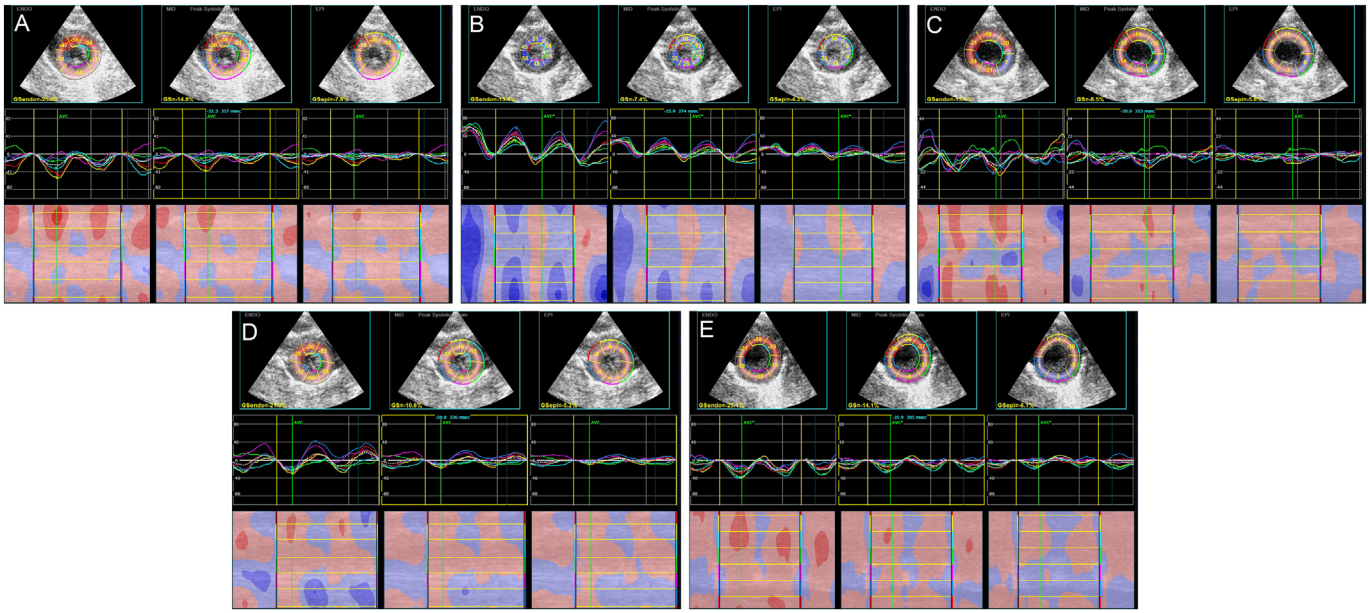

Fig. 3. Examples of left ventricular layer-specific circumferential strain assessed by Speckle Tracking Echocardiography. (A) Control group; (B) LPS group; (C) LPS + Nar_{50} group; (D) LPS + Nar_{100} group; (E) LPS + Dexa group. The endocardial, mid-myocardial and epicardial strain were arranged from left to right in each diagram.

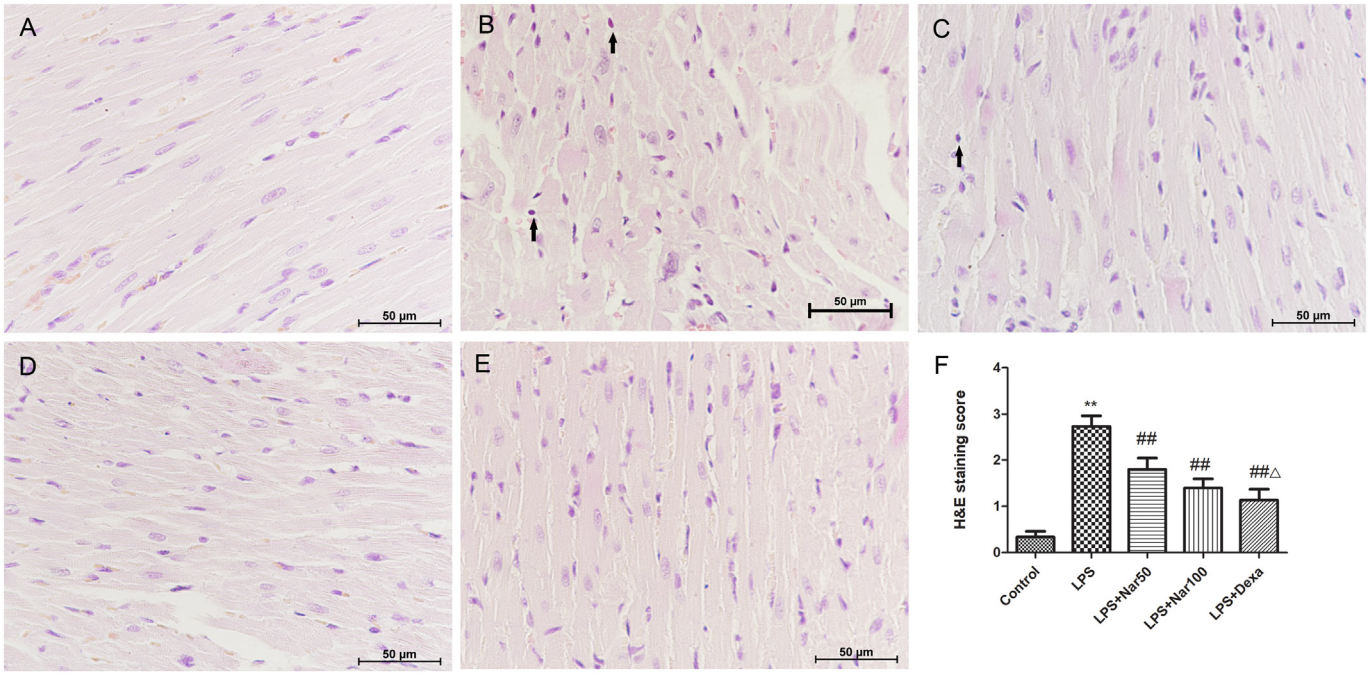

Fig. 4. Histopathologic changes of myocardial tissue observed among the five groups (light microscopy, HE × 400). (A) Control group; (B) LPS group; (C) LPS + Nar_{50} group; (D) LPS + Nar_{100} group; (E) LPS + Dexa group; (F) H&E staining score. Data were given as mean ± SD. $^{**}P < 0.01$ vs. control group; $^{\#\#}P < 0.01$ vs. LPS group; $^{\triangle}P < 0.05$ vs. LPS + Nar_{50} group. Arrows identified inflammatory cell infiltration.

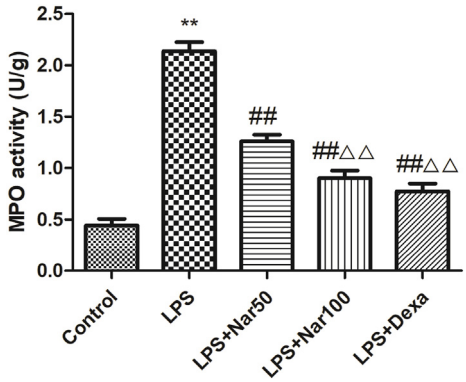

Fig. 5. Effects of Nar on MPO activity of LPS-induced SIMD in rats. Myocardial tissues were collected at 6 h after LPS treatment. Data were given as mean ± SD. $^{**}P < 0.01$ vs. control group; $^{\#\#}P < 0.01$ vs. LPS group; $^{\triangle\triangle}P < 0.01$ vs. LPS + Nar_{50} group.

protein was only detectable in the cytoplasm in the control group (Fig. 9A). After 6 h of LPS stimulation, NF-κB P65 was strongly expressed in the myocardial nucleus, with lighter staining of cytoplasm (Fig. 9B). The LPS + Nar groups, as well as the LPS + Dexa group, exhibited efficient suppression of NF-κB P65 expression (Fig. 9C–E). The IHC scores markedly increased following LPS stimulation, but significantly decreased following treatment with Nar and Dexa (Fig. 9F).

Fig. 10A shows the ratio of nucleus to cytoplasm (N/C) NF-κB p65 expression in LPS-induced SIMD rats. The results show that the N/C ratio of the LPS group was higher than that of the control group, and pretreatment with Nar and Dexa prevented p65 nuclear localization induced by LPS.

The expression of p-IκBα, p-NF-κB p65, and iNOS in H9c2 cardiomyocytes had increased rapidly by 24 h after LPS stimulation compared to the control group. However, Nar significantly suppressed the phosphorylation of NF-κB and the activation of iNOS after exposure to LPS (Fig. 10B).

To further explore the protective mechanism of Nar on cardiomyocytes, we tested whether the inhibition of NF-kB activation by Nar was mediated by the PI3K/AKT signaling pathway. H9c2 cardiomyocytes were treated with a selective PI3K inhibitor, LY294002. As shown in Fig. 10C, LY294002 blocked the phosphorylation of AKT induced by Nar in LPS-stimulated cardiomyocytes. The results in Fig. 10D show that the Nar-induced reduction of the NF-κB p65 N/C ratio was prevented by LY294002 treatment, demonstrating the need for PI3K/AKT activation. These findings strongly suggest that Nar induces AKT phosphorylation and prevents NF-κB p65 nuclear localization by activating the PI3K/AKT pathway.

4. Discussion

Sepsis is a serious clinical problem, and its poor prognosis is due to a severe systemic inflammatory response, which may lead to cardiac dysfunction. In the present study, we used LPS induction to establish an SIMD model, which was used to evaluate the effect of Nar on the PI3K/AKT/NF-κB signaling pathway in vivo and in vitro. The results demonstrated that Nar improved cardiac function, mitigated the expression of myocardial injury enzymes, and reduced the infiltration of inflammatory cells and the production of inflammatory cytokines. Furthermore, PI3K/AKT inhibition partially abolished the effects of Nar on NF-κB nuclear translocation. Our data suggest that Nar effectively attenuated LPS-induced acute myocardial injury by activating the PI3K/AKT pathway and inhibiting NF-κB signaling pathway.

This is the first study that analyzes layer-specific myocardial strain to evaluate the protective effect of Nar on SIMD. The rat myocardium is divided into three layers: the endocardial, mid-myocardial, and epicardial layers; and the myocardium contains fibers extending in different directions: longitudinal, circumferential, radial direction, and rotation. STE can grade each segment automatically according to the tracking quality of a scale and can then recognize myocardial dysfunction in different myocardial axes [16,29]. Li reported that STE can detect abnormal myocardial contractility at the early stage of sepsis when LPS does not affect LVEDd, LVEDs, LVEF, or FS [30]. However, their study focused on global strain without further distinction of the

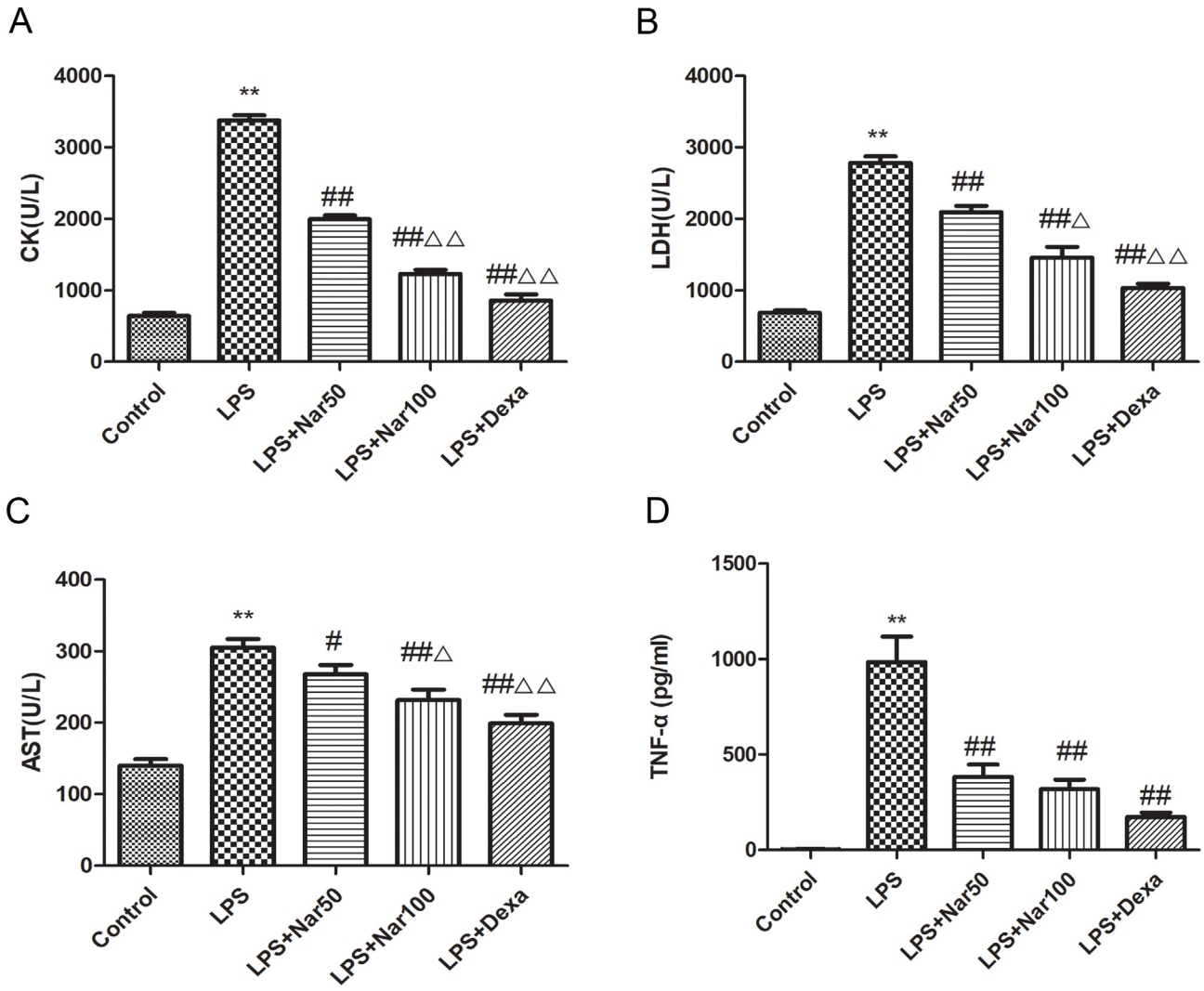

Fig. 6. The effect of Nar on myocardial enzymes and inflammatory cytokine in serum. Values were expressed as mean ± SD. $^{**}P < 0.01$ vs. the control group; $^{\#}P < 0.05$, $^{\#\#}P < 0.01$ vs. the LPS group; $^{\triangle}P < 0.05$, $^{\triangle\triangle}P < 0.01$ vs. the LPS + Nar_{50} group.

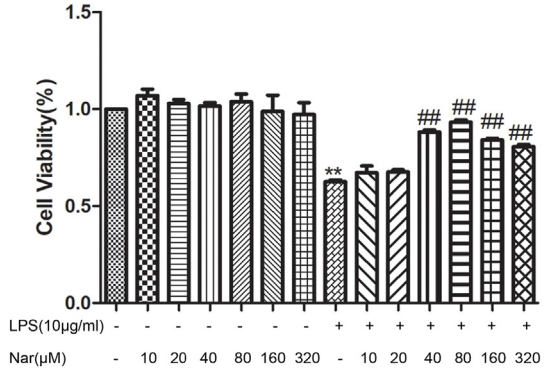

Fig. 7. Effect of Nar on H9c2 cardiomyocytes viability. H9c2 cardiomyocytes were incubated in the presence or absence of Nar (10, 20, 40, 80, 160, and 320 μM) and LPS (10 μg/ml) for 24 h. After that, cell viability was determined with CCK-8 assay. Data are presented as mean ± SD of three independent experiments. $^{**}P < 0.01$ vs. control group; $^{\#\#}P < 0.01$ vs. LPS group.

different layers of left ventricle. In this study, layer-specific analysis revealed that all three layers of LS and CS significantly decreased in LPS group, and the highest strain existed in endocardial layer while the lowest was in the epicardial layer. The most prominent decrease in myocardial strain was seen in the endocardial layer, which is the most susceptible to ischemic injury [31]. Liu found that LS-endo and LSr-endo were superior to global strain in predicting viable myocardium in acute non-transmural myocardial infarction [32]. We also found that the most serious damage occurred in the endocardial layer. Layer-specific myocardial strain analysis may increase the diagnostic accuracy of myocardial function in preeclampsia patients [18]. In this study, it aided in diagnosis of myocardial dysfunction in SIMD and allowed us to evaluate the protective effect of Nar. Pretreatment with Nar significantly decreased the myocardial strain and strain rate induced by LPS. This suggests that Nar can protect rats from LPS-induced myocardial injury.

The pathogenesis of SIMD is complex, and inflammatory mediators play important roles in cardiac insufficiency [33]. After LPS challenge, SD rats showed inflammatory cell infiltration into the heart, decreased myocardial systolic function, and elevated levels of pro-inflammatory cytokines. These pathological changes are consistent with previous studies [34,35]. MPO activity, a major marker of neutrophil infiltration, is used for assessing the intensity of inflammation [36]. In the present study, LPS treatment caused a large increase in MPO activity in the myocardial tissue. Nar treatment not only alleviated the pathological damage and preserved myocardial structural integrity, but also inhibited the activity of MPO. CK, LDH, and AST are closely related to myocardial tissue injury and serve as markers of abnormal myocardial

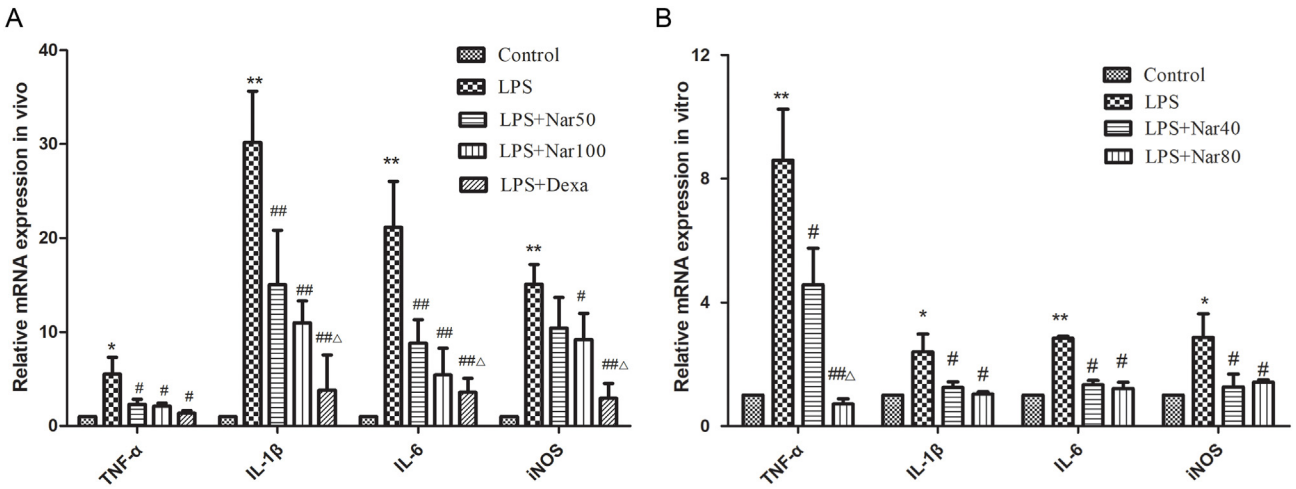

Fig. 8. Effect of Nar on the mRNA expressions of TNF-α, IL-1β, IL-6, and iNOS in vivo (A) and in vitro (B). Data were given as mean ± SD. $^{*}P < 0.05$ and $^{**}P < 0.01$ vs. control group; $^{\#}P < 0.05$ and $^{\#\#}P < 0.01$ vs. LPS group; $^{\triangle}P < 0.05$ vs. LPS + Nar_{50} group.

energy metabolism and myocardial necrosis [22]. These enzymes are found in almost all tissues, with the highest amounts in the myocardium. When a small amount of tissue is damaged, the enzymes are released into the circulation to increase the vitality in the blood [14]. In this study, Nar treatment significantly reduced the levels of myocardial enzymes in the serum. Previous studies have shown that Nar can mitigate the inflammatory response in PFOS-induced liver injury [37] and can also effectively mitigate lung inflammation in acrolein-induced pulmonary injury by modulating the MAPK, p53, and NF-κB signaling pathways [38]. In this study, Nar decreased the levels of pro-inflammatory cytokines in LPS-induced myocardial dysfunction, which suggests that the myocardial protective functions of Nar are associated with anti-inflammatory effects.

It has been reported that Nar can inhibit inflammation and inflammatory factors [9]. In this study, we found that Nar did not reduce cardiomyocytes cell viability, but did significantly attenuate of LPS-induced cell toxicity. LPS activates the NF-κB pathway and can also stimulate the transcription and expression of inflammatory cytokines in multiple cell lines [39]. NF-κB plays a pivotal role in the development of inflammation. After LPS stimulation, NF-κB is liberated due to phosphorylation and degradation of the inhibitor of NF-κB protein (IκB) and subsequently translocates into the nucleus [40]. NF-κB can then activate many inflammatory genes, including TNF-α, interleukin 1β (IL-1β), interleukin 6 (IL-6), and inducible nitric oxide synthase (iNOS) [15]. Increased inflammatory cytokine production may further stimulate activation of the NF-κB signaling pathway, leading to further release of cytokines and oxidative mediators [41]. LPS, IL-1β, and TNF-α have been shown to increase the production of iNOS, which inhibits cardiac contractility [13,30]. Previous studies have shown that Nar can inhibit the deterioration of cisplatin-induced renal injury in rats by reducing NF-κB and iNOS expression [42]. Furthermore, many agents protect mice against SIMD by inhibiting the NF-κB signaling pathway [43]. Therefore, we investigated whether Nar protected rats against SIMD by regulating the NF-κB signaling pathway. We found that Nar

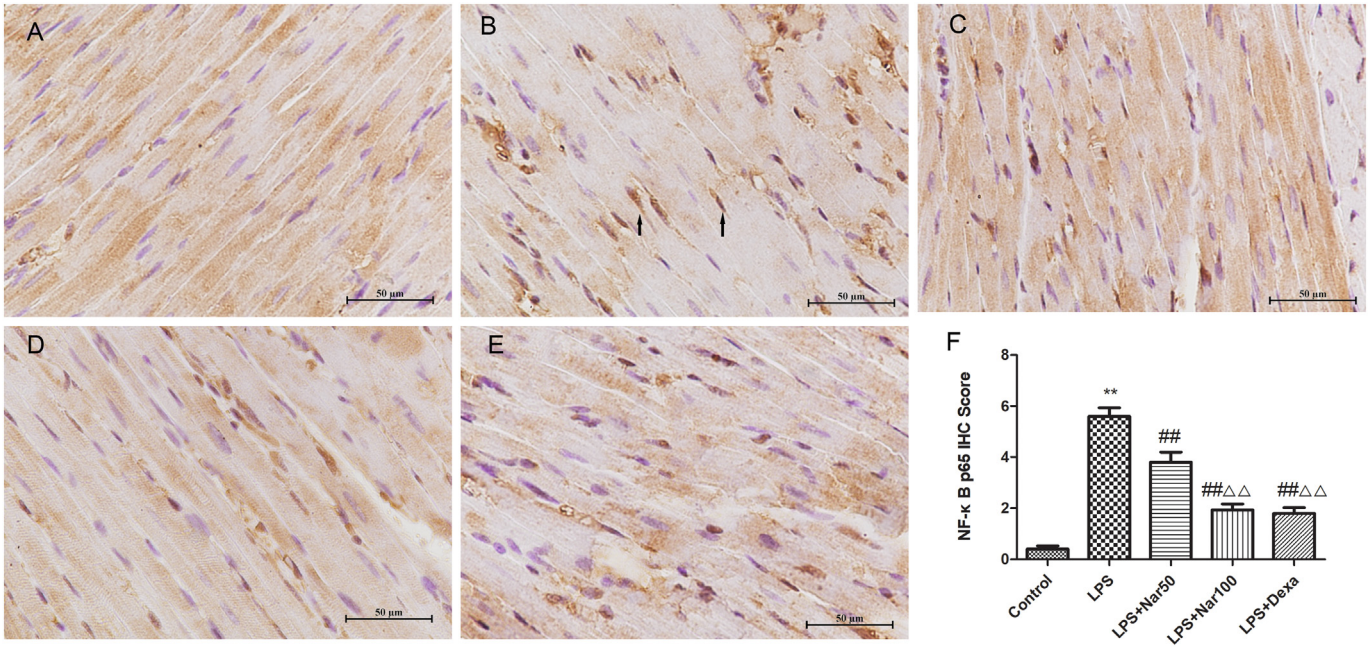

Fig. 9. The effect of Nar on the protein level of NF-κB against LPS induced cardiac injure in SIMD rats. (A) Control group; (B) LPS group; (C) LPS + Nar_{50} group; (D) LPS + Nar_{100} group; (E) LPS + Dexa group (original magnification ×400); (F) Immunohistochemical scores of NF-κB p65. Arrows identified positive staining cells. Data were given as mean ± SD. $^{**}P < 0.01$ vs. control group; $^{\#\#}P < 0.01$ vs. LPS group. $^{\triangle\triangle}P < 0.01$ vs. LPS + Nar_{50} group.

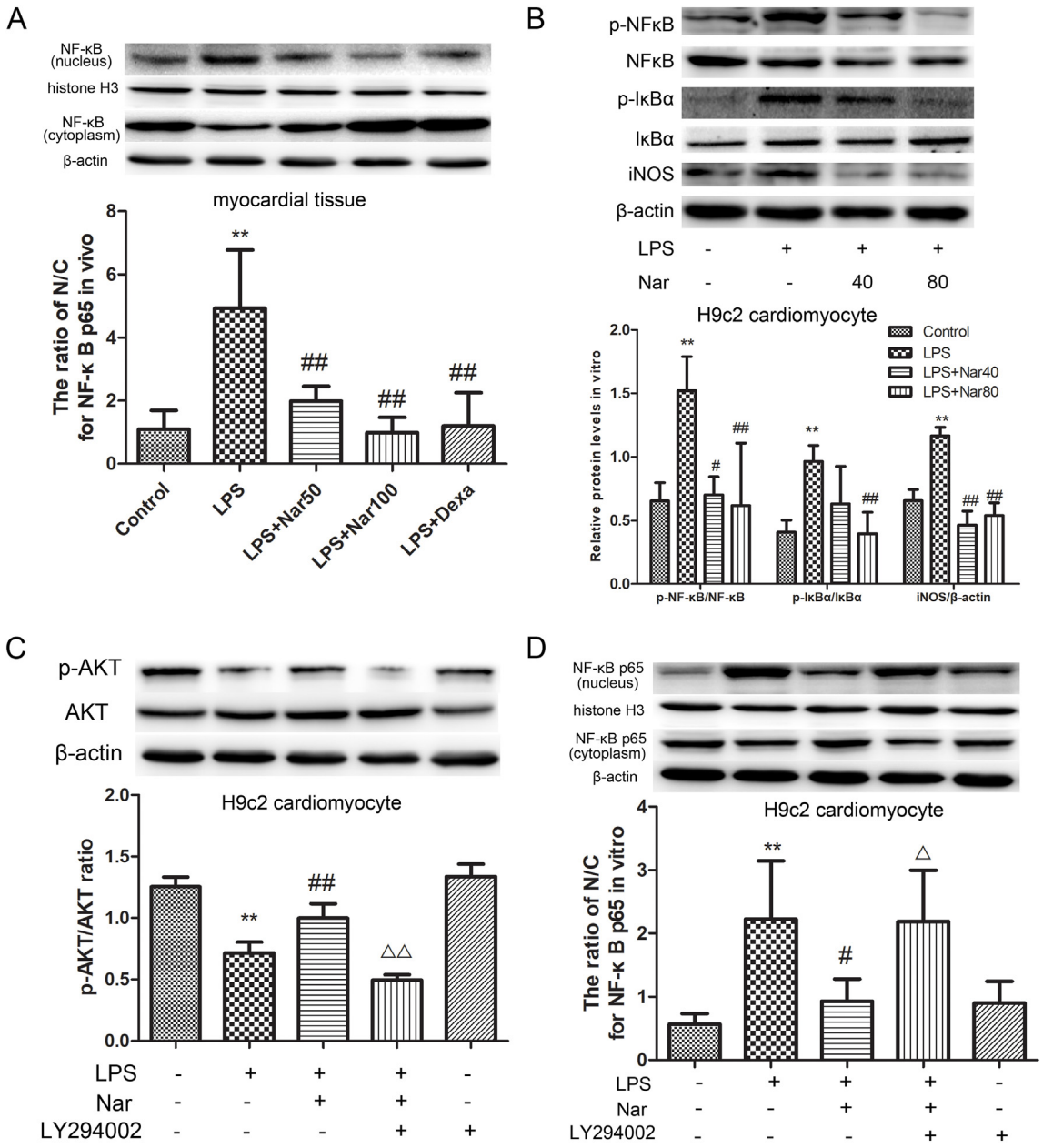

Fig. 10. The effect of Nar on the protein level of PI3K/AKT/NF-κB Pathway against LPS-induced cardiac injure in vivo and in vitro. (A) The expression of NF-κB in the nuclei and cytoplasm of heart tissue in rats after 6 h of LPS-induced SIMD. (B) The H9c2 cardiomyocytes were pre-treated with Nar (40/80 μM) for 1 h and then stimulated with LPS (10 μg/ml) for 24 h. (C) The expression of p-AKT and AKT in LPS-induced H9c2 cardiomyocytes. Cells were pretreated with Nar (80 μM) and LY294002 (10 μM) for 1 and 2 h respectively before stimulation with LPS (10 μg/ml) for 24 h. (D) The expression of NF-κB in the nuclei and cytoplasm of H9c2 cardiomyocytes. Cells were pretreated with Nar (80 μM) and LY294002 (10 μM) for 1 and 2 h respectively before stimulation with LPS (10 μg/ml) for 24 h. Data were given as mean ± SD. $^{**}P < 0.01$ vs. the control group; $^{\#}P < 0.05$, $^{\#\#}P < 0.01$ vs. the LPS group. $^{\triangle}P < 0.05$, $^{\triangle\triangle}P < 0.01$ vs. LPS + Nar group.

treatment prevented the phosphorylation of NF-κB and IκB, and that it inhibited the activation of iNOS after exposure to LPS. The PI3K/AKT pathway has been known to play essential roles in the regulation of various biological processes including cellular apoptosis, proliferation and survival [14]. Recently, many studies have demonstrated that the activation of AKT by phosphorylation can negatively regulate the NF-κB pathway and limiting pro-inflammatory responses in vitro and in vivo [15,44]. Therefore, we have examined whether the inhibition of NF-κB activation by Nar is mediated via the PI3K/AKT pathway. In this study, the ratio of nucleus to cytoplasm for NF-κB in the LPS + Nar group was significantly lower than that in the LPS group in vitro and in vivo, while treatment with the PI3K inhibitor LY294002 reversed the decrease in NF-κB nuclear translocation and the increase in p-AKT after Nar treatment in H9c2 cardiomyocytes. These results suggest that Nar exhibits its protective effect on LPS-induced SIMD through the PI3K/AKT/NF-κB signaling pathway.

In conclusion, pretreatment with Nar can alleviate the decrease of global and layer-specific myocardial strain in SIMD rats by reducing the secretion of pro-inflammatory cytokines, activating PI3K/AKT pathway, and inhibiting NF-κB phosphorylation and nuclear translocation. These findings show that Nar may have an anti-inflammatory protective effect on LPS-induced myocardial injury.

Funding

This study was supported by the Foundation for Innovative

Research Groups of the National Natural Science Foundation of China (No. 81571686).

Declaration of Competing Interest

The authors declare that there are no conflicts of interest concerning this article.

Acknowledgments

The authors thank Yajun Wang, He Zhang and all the teachers in Experimental Center, Shengjing Hospital.

References

[1] M. Singer, C.S. Deutschman, C.W. Seymour, M. Shankar-Hari, D. Annane, M. Bauer, et al., The third international consensus definitions for sepsis and septic shock (Sepsis-3), JAMA 315 (8) (2016) 801–810.
[2] F.J. Romero-Bermejo, M. Ruiz-Bailen, J. Gil-Cebrian, M.J. Huertos-Ranchal, Sepsis-induced cardiomyopathy, Curr. Cardiol. Rev. 7 (3) (2011) 163–183.
[3] A. Vieillard-Baron, Septic cardiomyopathy, Ann. Intensive Care 1 (2011) 6.
[4] M.W. Merx, C. Weber, Sepsis and the heart, Circulation 116 (7) (2007) 793–802.
[5] R. Chen, Q.L. Qi, M.T. Wang, Q.Y. Li, Therapeutic potential of naringin: an overview, Pharm. Biol. 54 (12) (2016) 3203–3210.
[6] J.J. Peterson, J.T. Dwyer, P.F. Jacques, M.L. McCullough, Associations between flavonoids and cardiovascular disease incidence or mortality in European and US populations, Nutr. Rev. 70 (9) (2012) 491–508.
[7] F. Chen, N. Zhang, X. Ma, T. Huang, Y. Shao, C. Wu, et al., Naringin alleviates diabetic kidney disease through inhibiting oxidative stress and inflammatory reaction, PLoS One 10 (11) (2015) e0143868.
[8] A. Visnagri, M. Adil, A.D. Kandhare, S.L. Bodhankar, Effect of naringin on hemodynamic changes and left ventricular function in renal artery occluded renovascular hypertension in rats, J. Pharm. Bioallied Sci. 7 (2015) 121–127.
[9] Hsueh TP, Sheen JM, Pang JH, Bi KW, Huang CC, Wu HT, et al. The anti-atherosclerotic effect of naringin is associated with reduced expressions of cell adhesion molecules and chemokines through NF-κB pathway. Molecules. 21 (2) (2016) pii: E195.
[10] N. Rani, S. Bharti, M. Manchanda, T.C. Nag, R. Ray, S.S. Chauhan, et al., Regulation of heat shock proteins 27 and 70, p-Akt/p-eNOS and MAPKs by naringin dampens myocardial injury and dysfunction in vivo after ischemia/reperfusion, PLoS One 8 (12) (2013) e82577.
[11] Q. You, Z. Wu, B. Wu, C. Liu, R. Huang, L. Yang, et al., Naringin protects cardiomyocytes against hyperglycemia-induced injuries in vitro and in vivo, J. Endocrinol. 230 (2) (2016) 197–214.
[12] L. Xianchu, P.Z. Lan, L. Qiufang, L. Yi, R. Xiangcheng, H. Wenqi, et al., Naringin protects against lipopolysaccharide-induced cardiac injury in mice, Environ. Toxicol. Pharmacol. 48 (2016) 1–6.
[13] S. Alvarez, T. Vico, V. Vanasco, Cardiac dysfunction, mitochondrial architecture, energy production, and inflammatory pathways: interrelated aspects in endotoxemia and sepsis, Int J Biochem Cell Biol. 81(Pt B) (2016) 307–314.
[14] L. Chen, P. Liu, X. Feng, C. Ma, Salidroside suppressing LPS-induced myocardial injury by inhibiting ROS-mediated PI3K/Akt/mTOR pathway in vitro and in vivo, J. Cell. Mol. Med. 21 (12) (2017) 3178–3189.
[15] S. Franceschelli, M. Pesce, A. Ferrone, D.M. Gatta, A. Patruno, M.A. Lutiis, et al., Biological effect of licochalcone C on the regulation of PI3K/Akt/eNOS and NF-κB/iNOS/NO signaling pathways in H9c2 cells in response to LPS stimulation, Int. J. Mol. Sci. 18 (4) (2017) (pii: E690).
[16] R. Kramann, J. Erpenbeck, R.K. Schneider, A.B. Röhl, M. Hein, V.M. Brandenburg, et al., Speckle tracking echocardiography detects uremic cardiomyopathy early and predicts cardiovascular mortality in ESRD, J. Am. Soc. Nephrol. 25 (10) (2014) 2351–2365.
[17] M. Yamada, K. Takahashi, M. Kobayashi, K. Yazaki, H. Takayasu, K. Akimoto, et al., Mechanisms of left ventricular dysfunction assessed by layer-specific strain analysis in patients with repaired tetralogy of Fallot, Circ. J. 81 (6) (2017) 846–854.
[18] J. Cong, Y. Lee, X. Fu, Z. Wang, W. Wang, J. Lee, Quantitative evaluation of longitudinal strain in layer-specific myocardium in patients with preeclampsia, Int. J. Card. Imaging 34 (2) (2018) 193–200.
[19] S.A. Tavener, E.M. Long, S.M. Robbins, K.M. McRae, H. Van Remmen, P. Kubes, et al., Immune cell toll-like receptor 4 is required for cardiac myocyte impairment during endotoxemia, Circ. Res. 95 (7) (2004) 700–707.
[20] W. You, X. Min, X. Zhang, B. Qian, S. Pang, Z. Ding, et al., Cardiac-specific expression of heat shock protein 27 attenuated endotoxin-induced cardiac dysfunction and mortality in mice through a PI3K/Akt-dependent mechanism, Shock 32 (1) (2009) 108–117.
[21] C. Caglayan, Y. Temel, F.M. Kandemir, S. Yildirim, S. Kucukler, Naringin protects against cyclophosphamide-induced hepatotoxicity and nephrotoxicity through modulation of oxidative stress, inflammation, apoptosis, autophagy, and DNA damage, Environ. Sci. Pollut. Res. Int. 25 (21) (2018) 20968–20984.
[22] H. He, X. Chang, J. Gao, L. Zhu, M. Miao, T. Yan, Salidroside mitigates sepsis-induced myocarditis in rats by regulating IGF-1/PI3K/Akt/GSK-3β signaling, Inflammation 38 (6) (2015) 2178–2184.
[23] Z. Wei, G. Yang, R. Xu, C. Zhu, F. He, Q. Dou, et al., Correlation between protein 4.1R and the progression of heart failure in vivo, Genet. Mol. Res. 15 (2) (2016) (gmr.15028648).
[24] M. Zhou, W. Xu, J. Wang, J. Yan, Y. Shi, C. Zhang, et al., Boosting mTOR-dependent autophagy via upstream TLR4-MyD88-MAPK signaling and downstream NF-κB pathway quenches intestinal inflammation and oxidative stress injury, EBioMedicine 35 (2018) 345–360.
[25] J. Chen, R. Guo, H. Yan, L. Tian, Q. You, S. Li, et al., Naringin inhibits ROS-activated MAPK pathway in high glucose-induced injuries in H9c2 cardiac cells, Basic Clin. Pharmacol. Toxicol. 114 (4) (2014) 293–304.
[26] H.F. Deng, X.L. Wang, H. Sun, X.Z. Xiao, Puerarin inhibits expression of tissue factor induced by oxidative low-density lipoprotein through activating the PI3K/Akt/eNOS pathway and inhibiting activation of ERK1/2 and NF-κB, Life Sci. 191 (2017) 115–121.
[27] A. Kalmár, B. Wichmann, O. Galamb, S. Spisák, K. Tóth, K. Leiszter, et al., Gene-expression analysis of a colorectal cancer-specific discriminatory transcript set on formalin-fixed, paraffin-embedded (FFPE) tissue samples, Diagn. Pathol. 10 (2015) 126.
[28] Y. Wang, J. Tan, H. Du, X. Liu, S. Wang, S. Wu, et al., Notch1 inhibits rosiglitazone-induced adipogenic differentiation in primary thymic stromal cells, Front. Pharmacol. 9 (2018) 1284.
[29] X.X. Luo, Y. Zhu, Y. Sun, Q. Ge, J. Su, H.K. So, et al., Does masked hypertension cause early left ventricular impairment in youth? Front. Pediatr. 6 (2018) 167.
[30] T. Li, J.J. Liu, W.H. Du, X. Wang, Z.Q. Chen, L.C. Zhang, 2D speckle tracking imaging to assess sepsis induced early systolic myocardial dysfunction and its underlying mechanisms, Eur. Rev. Med. Pharmacol. Sci. 18 (20) (2014) 3105–3114.
[31] S.I. Sarvari, K.H. Haugaa, W. Zahid, B. Bendz, S. Aakhus, L. Aaberge, et al., Layer-specific quantification of myocardial deformation by strain echocardiography may reveal significant CAD in patients with non-ST-segment elevation acute coronary syndrome, JACC Cardiovasc. Imaging 6 (5) (2013) 535–544.
[32] K. Liu, Y. Wang, Q. Hao, G. Li, P. Chen, D. Li, Evaluation of myocardial viability in patients with acute myocardial infarction: layer-specific analysis of 2-dimensional speckle tracking echocardiography, Medicine (Baltimore) 98 (3) (2019) e13959.
[33] K. Drosatos, A. Lymperopoulos, P.J. Kennel, N. Pollak, P.C. Schulze, I.J. Goldberg, Pathophysiology of sepsis-related cardiac dysfunction: driven by inflammation, energy mismanagement, or both? Curr. Heart Fail. Rep. 12 (2) (2015) 130–140.
[34] H. Zhao, M. Zhang, F. Zhou, W. Cao, L. Bi, Y. Xie, et al., Cinnamaldehyde ameliorates LPS-induced cardiac dysfunction via TLR4-NOX4 pathway: the regulation of autophagy and ROS production, J. Mol. Cell. Cardiol. 101 (2016) 11–24.
[35] A.E. Khodir, H.A. Ghoneim, M.A. Rahim, G.M. Suddek, Montelukast attenuates lipopolysaccharide-induced cardiac injury in rats, Hum. Exp. Toxicol. 35 (4) (2016) 388–397.
[36] S. Abbaszadeh, A. Javidmehr, B. Askari, P.M.L. Janssen, H. Soraya, Memantine, an NMDA receptor antagonist, attenuates cardiac remodeling, lipid peroxidation and neutrophil recruitment in heart failure: a cardioprotective agent? Biomed. Pharmacother. 108 (2018) 1237–1243.
[37] Z. Lv, W. Wu, S. Ge, R. Jia, T. Lin, Y. Yuan, et al., Naringin protects against perfluorooctane sulfonate-induced liver injury by modulating NRF2 and NF-κB in mice, Int. Immunopharmacol. 65 (2018) 140–147.
[38] J.K. Kim, J.H. Park, H.J. Ku, S.H. Kim, Y.J. Lim, J.W. Park, et al., Naringin protects acrolein-induced pulmonary injuries through modulating apoptotic signaling and inflammation signaling pathways in mice, J. Nutr. Biochem. 59 (2018) 10–16.
[39] J.W. Lee, W. Chun, O.K. Kwon, H.A. Park, Y. Lim, J.H. Lee, et al., 3,4,5-Trihydroxycinnamic acid attenuates lipopolysaccharide (LPS)-induced acute lung injury via downregulating inflammatory molecules and upregulating HO-1/AMPK activation, Int. Immunopharmacol. 64 (2018) 123–130.
[40] P. Yang, Y. Han, L. Gui, J. Sun, Y.L. Chen, R. Song, et al., Gastrodin attenuation of the inflammatory response in H9c2 cardiomyocytes involves inhibition of NF-κB and MAPKs activation via the phos-phatidylinositol 3-kinase signaling, Biochem. Pharmacol. 85 (8) (2013) 1124–1133.
[41] Y. Lu, D. Xu, J. Liu, L. Gu, Protective effect of sophocarpine on lipopolysaccharide-induced acute lung injury in mice, Int. Immunopharmacol. 70 (2019) 180–186.
[42] Y. Chtourou, B. Aouey, S. Aroui, M. Kebieche, H. Fetoui, Anti-apoptotic and anti-inflammatory effects of naringin on cisplatin-induced renal injury in the rat, Chem. Biol. Interact. 243 (2016) 1–9.
[43] J. Zhai, Y. Guo, Paeoniflorin attenuates cardiac dysfunction in endotoxemic mice via the inhibition of nuclear factor-κB, Biomed. Pharmacother. 80 (2016) 200–206.
[44] G. Kulasekaran, S. Ganapasam, Neuroprotective efficacy of naringin on 3-nitropropionic acid-induced mitochondrial dysfunction through the modulation of Nrf2 signaling pathway in PC12 cells, Mol. Cell. Biochem. 409 (1–2) (2015) 199–211.